Cholecystectomy-related gut microbiota dysbiosis exacerbates colorectal tumorigenesis

Bo Tang, Shengpeng Li, Xin Li, Jialin He, An Zhou, Lingyi Wu, Xu Xiao, Sumin Wang, Hongfei Jiang, Jincheng Jian, Zhanjie Hou, Yusong Ge, Yuanyuan Lei, Jianchun Zhou, Dianji Tu, Cheng Lu, Min Yang, Shiming Yang

Table of contents

Supplementary Figures

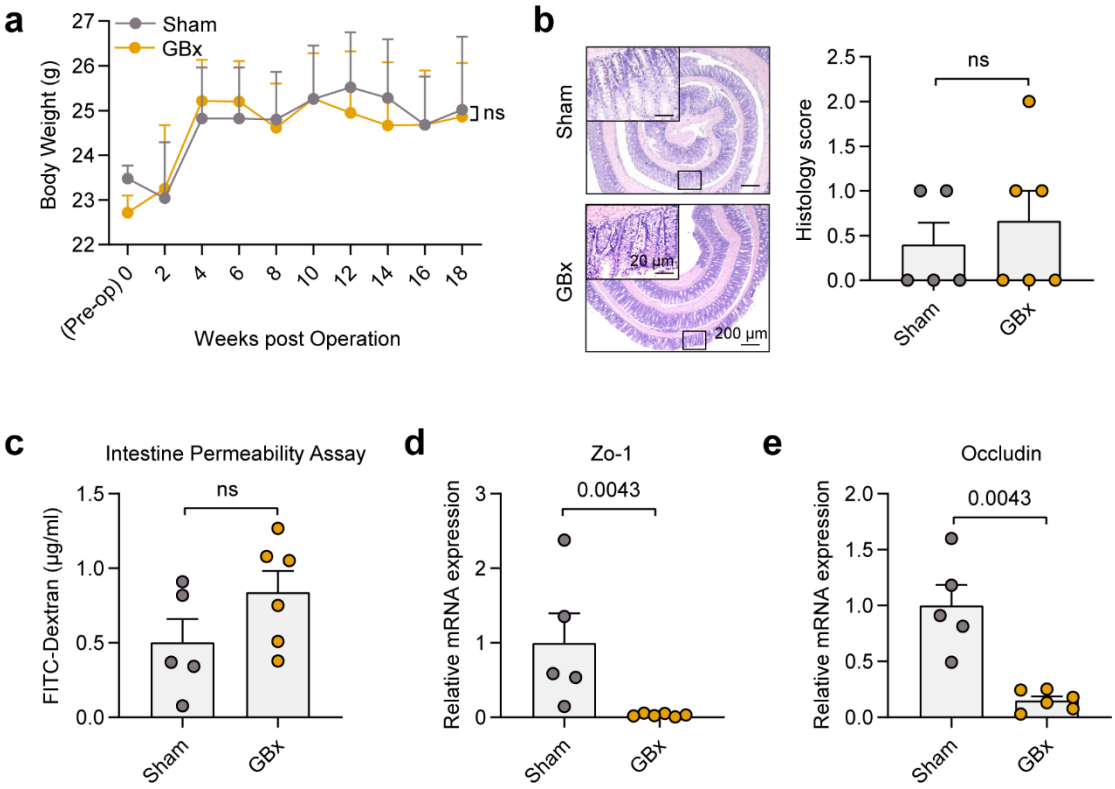

Supplementary Fig. 1. Changes in gut barrier function and epithelial integrity induced by cholecystectomy in mice. a The body weight of mice during the experimental period (Mann Whitney *U* test was used at the end point). **b** Representative H&E staining images and histology scores in mice after operation. The bottom scale bar is 200 μm and the top scale bar is 20 μm. **c** Intestinal permeability measured by FITC-dextran in mice after operation. **d, e** Relative expression of Zo-1 (**d**) and Occludin (**e**) in colon tissues from Sham and GBx mice. n = 5 vs 6. Data are shown as the mean ± SEM. P values were determined by two-tailed Mann Whitney U test and were indicated in each figure. ns, not significant; GBx, cholecystectomy; FITC-dextran, fluorescein isothiocyanate (FITC)-conjugated dextran; ZO-1, tight junction protein 1. Source data are provided as a Source Data file.

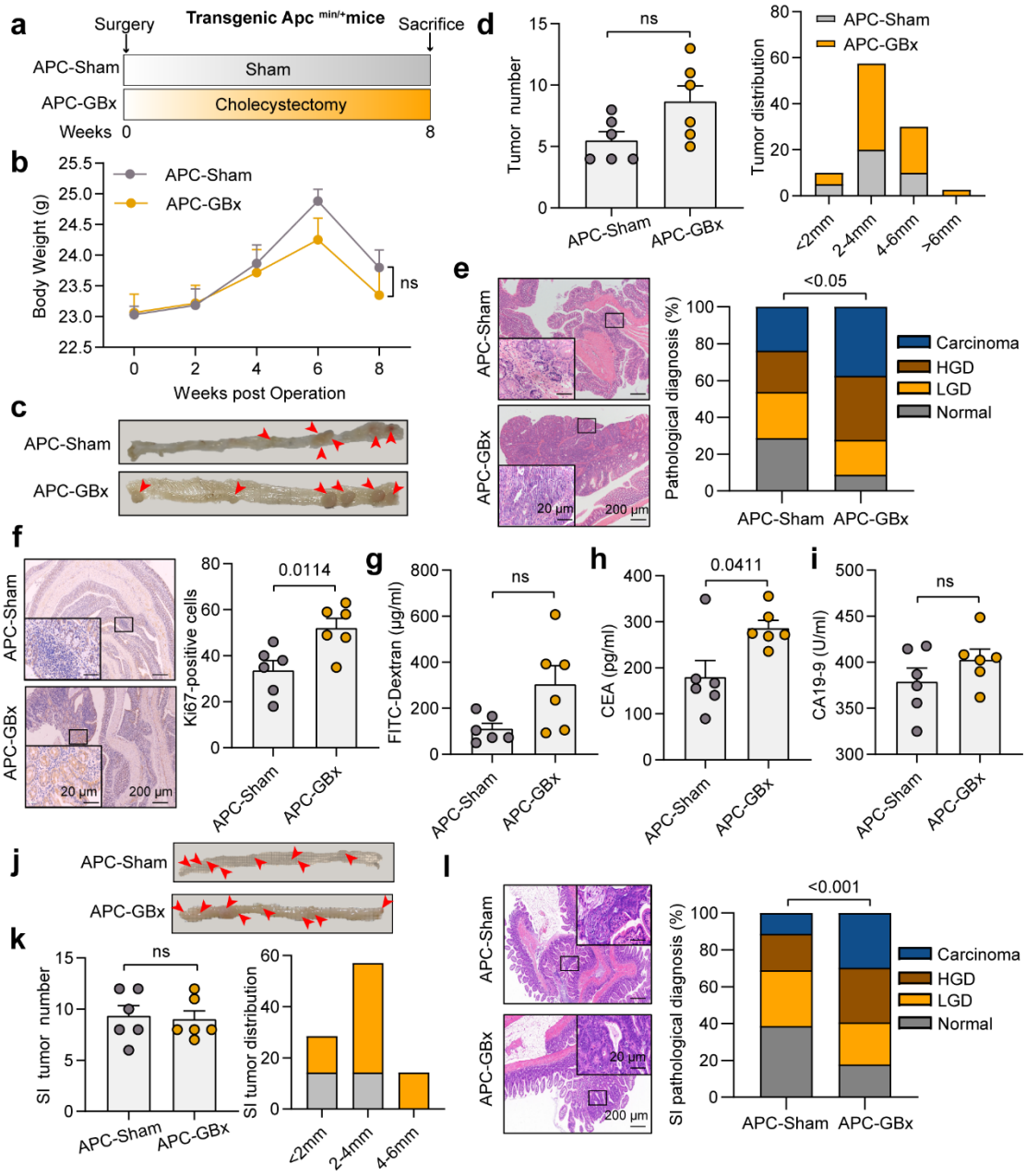

Supplementary Fig. 2. Cholecystectomy facilitates colorectal tumorigenesis in APC$^{min/+}$ mice. a Schematic overview of the treatments in the APC$^{min/+}$ mouse model following cholecystectomy. **b** The body weight of mice throughout the experimental period (two-tailed Mann Whitney *U* test was used at the end point). **c** Representative images of the colon in APC$^{min/+}$ mice. **d** Average tumor number (left) and tumor size distribution (right) in APC$^{min/+}$ mice within the sham or cholecystectomy group. **e** Representative images of H&E staining (left) and semiquantitative analysis of the

pathological score (right) in $APC^{min/+}$ mice (ANOVA). H&E staining showed normal, dysplastic mucosae and carcinoma in the colon tissues. The bottom scale bar is 200 μm and the top scale bar is 20 μm. **f** Representative images of Ki67 staining of mouse colons and semiquantitative analysis. The bottom scale bar is 200 μm and the top scale bar is 20 μm. **g** Intestinal permeability measured by FITC-dextran in the above mice (two-tailed Welch's *t* test). **h, i** Serum levels of CEA (**h**, two-tailed Mann-Whitney *U* test) and CA19-9 (**i**) in mice. **j** Representative images of the intestine of $APC^{min/+}$ mice at sacrifice. **k** Average tumor number (left) and tumor size distribution (right) in intestine of $APC^{min/+}$ mice. **l** Representative images of H&E staining (left) and semiquantitative analysis of the pathological score (right) in the intestine of $APC^{min/+}$ mice (ANOVA). H&E staining showed normal, dysplastic mucosae and carcinoma in the colon tissues. The bottom scale bar is 200 μm and the top scale bar is 20 μm. n = 6/group. Data are shown as the mean ± SEM. *P* values were determined by two-tailed *t* test for **d**, **f**, **i**, **k**, and were indicated in each figure. GBx, Cholecystectomy; CEA, carcinoembryonic antigen; CA19-9, cancer antigen 19-9; APC, adenomatous polyposis coli; ns, not significant; SI, small intestine. Source data are provided as a Source Data file.

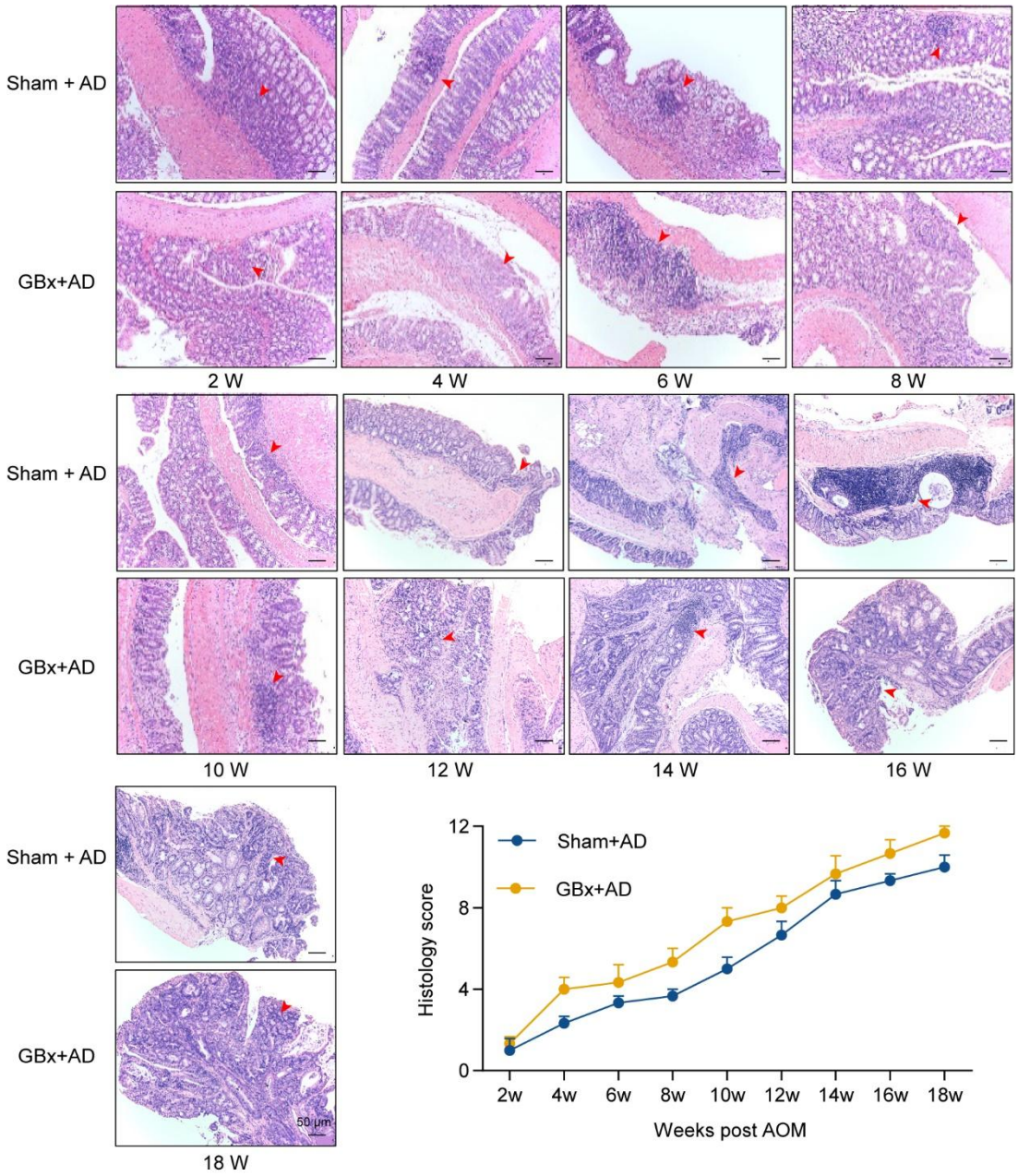

Supplementary Fig. 3. Cholecystectomy accelerates colorectal tumorigenesis during the experimental period, related to Fig. 2. Representative images of H&E staining and histology score of colon tissues of mice in different experimental periods. n = 3/group. The regions of the lesion were pointed out by red arrows. Scale bar, 50 μm. Source data are provided as a Source Data file.

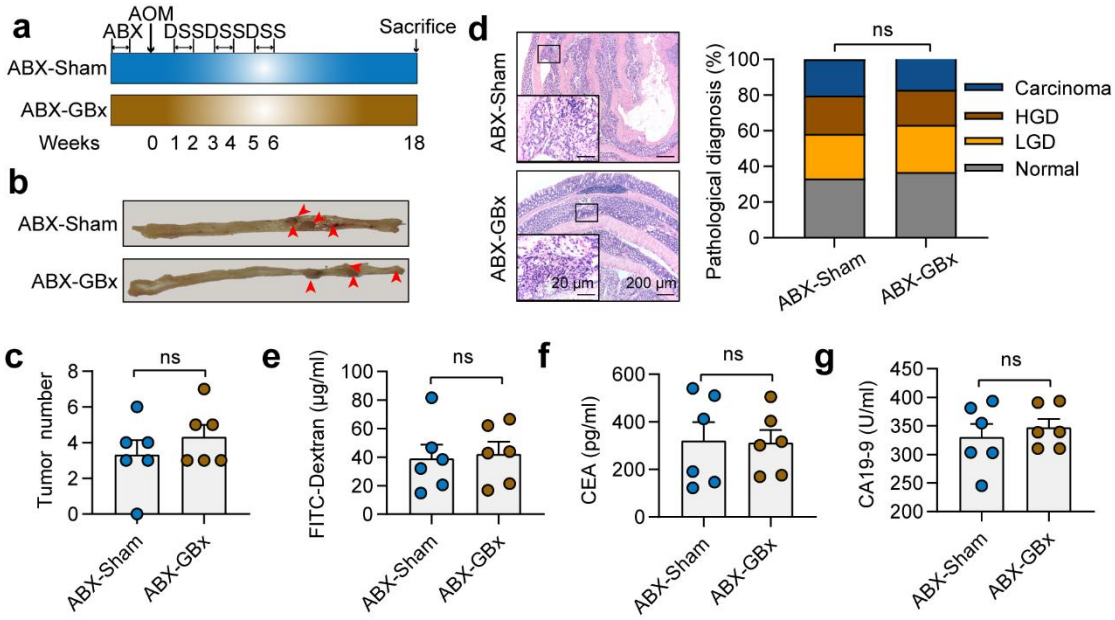

Supplementary Fig. 4. Indistinguishable colorectal tumorigenesis between ABX-Sham and ABX-GBx mice, related to Fig. 3. a Schematic overview of mouse ABX experiments in the C57BL/6J mouse model. **b** Representative images of the colon in the ABX experiments. **c** The average tumor number in mice in the ABX experiments (two-tailed Mann-Whitney *U* test). **d** Representative images of H&E staining and semiquantitative analysis in each group (ANOVA). H&E staining showed normal, dysplastic mucosae and carcinoma in the colon tissues. The bottom scale bar is 200 μm and the top scale bar is 20 μm. **e** Intestinal permeability measured by FITC-dextran. **f, g** Serum CEA (f) and CA19-9 (**g**) levels in mice in the ABX experiments. $n = 6$/group. Data are shown as the mean ± SEM. *P* values were determined by two-tailed *t* test for **e-g**, and were indicated in each figure. ns, not significant; ABX, antibiotic cocktail; AOM, azoxymethane; DSS, dextran sodium sulfate. Source data are provided as a Source Data file.

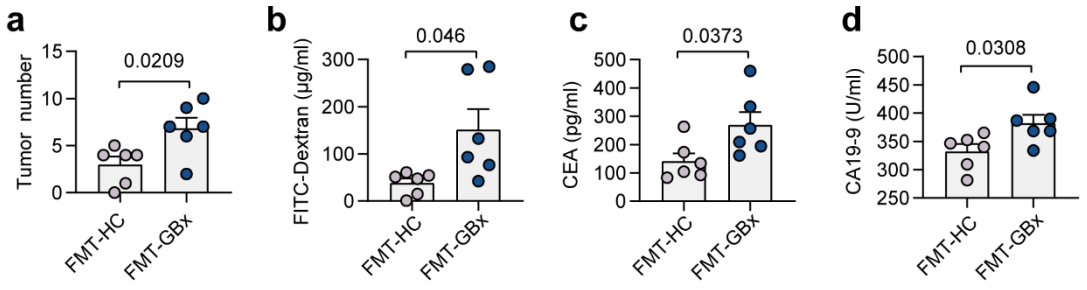

Supplementary Fig. 5. FMT derived from GBx patients promotes colorectal tumorigenesis, related to Fig. 3. a The average tumor number of the FMT recipient mice (two-tailed Mann-Whitney *U* test). **b** Intestinal permeability measured by FITC-dextran (two-tailed Welch's *t* test). **c, d** Serum CEA (**c**) and CA19-9 (**d**) levels in FMT recipient mice (two-tailed *t* test). $n = 6$/group. Data are shown as the mean ± SEM. P values are indicated on the top of each figure. All data were representative of more than three independent experiments. FMT, fecal microbiota transplantation; HC, healthy control. Source data are provided as a Source Data file.

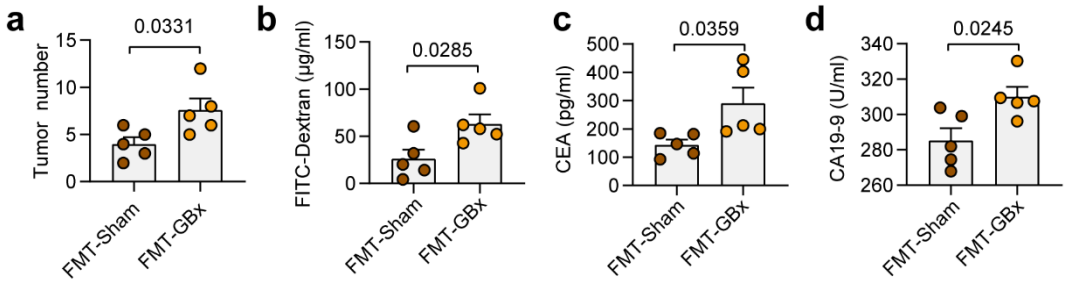

Supplementary Fig. 6. FMT derived from tumor-bearing GBx mice promotes colorectal tumorigenesis, related to Fig. 3. a The average tumor number of the FMT recipient mice (two-tailed Mann-Whitney *U* test). **b** Intestinal permeability measured by FITC-dextran. **c, d** Serum CEA (**c**) and CA19-9 (**d**) levels in FMT recipient mice. *n* = 5/group. Data are shown as the mean ± SEM. *P* values were determined by two-tailed *t* test for **b**-**d**, and were indicated in each figure. Source data are provided as a Source Data file.

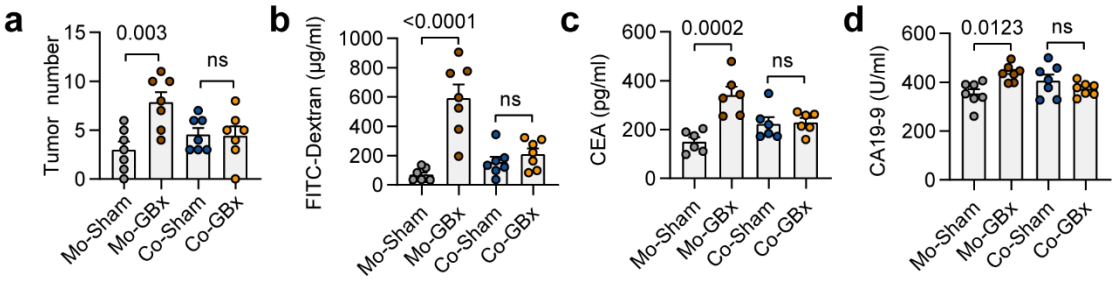

Supplementary Fig. 7. Tumor number, intestinal permeability, serum CEA and CA19-9 levels in mice after cohousing experiments, related to Fig. 3. a Average tumor number of the colon in the cohousing experiments. **b** Intestinal permeability measured by FITC-dextran. **c, d** Serum CEA (**c**) and CA19-9 (**d**) levels in mice in the cohousing experiments. $n = 7$/group. Data are shown as the mean ± SEM. *P* values were determined by ANOVA and were indicated in each figure. ns, not significant; Mo, mono-housed; Co, co-housed. Source data are provided as a Source Data file.

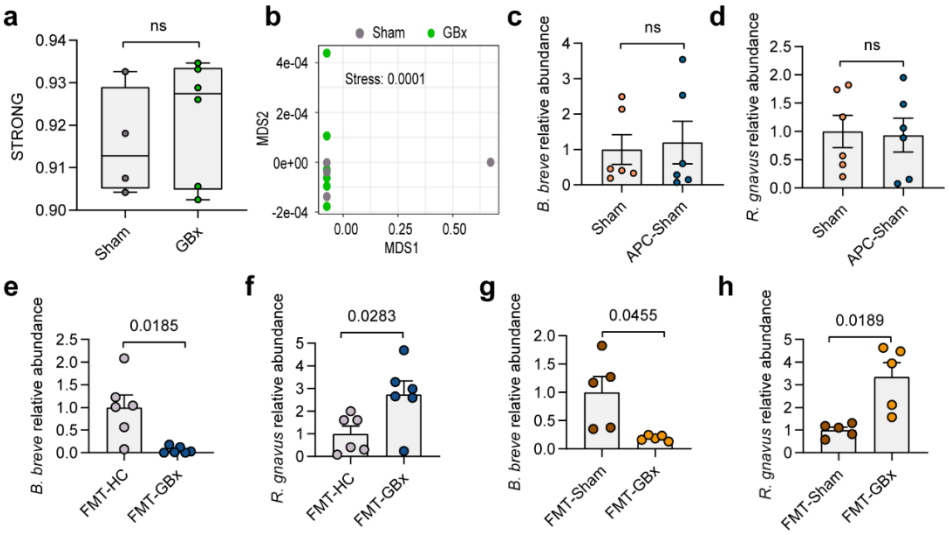

Supplementary Fig. 8. The gut microbiota diversity in Sham and GBx mice, and microbiota abundance in Sham, APC-Sham, and FMT mice models, related to Fig. 4. a Index (α-diversity) of the gut microbiota in Sham and GBx mice (two-tailed Mann-Whitney *U* test, *n* = 4 vs 6). The center line of the boxplot represents the median; the box spans from the first quartile (Q1) to the third quartile (Q3); the whiskers extend from the box to the maximum and minimum values within 1.5 times the interquartile range (IQR) from the box. **b** NMDS of bacterial communities based on Bray-Curtis similarity between Sham and GBx mice (*n* = 4 vs 6). **c** qPCR analysis of *B. breve* abundance in Sham and APC-Sham groups (two-tailed Mann-Whitney *U* test, *n* = 6/group). **d** qPCR analysis of *R. gnavus* abundance in Sham and APC-Sham groups (two-tailed *t* test, *n* = 6/group). **e** qPCR analysis of *B. breve* abundance after the FMT experiments (two-tailed Welch's *t* test, *n* = 6/group). **f** qPCR analysis of *R. gnavus* abundance between FMT-HC and FMT-GBx group (two-tailed *t* test, *n* = 6/group). **g, h** qPCR analysis of *B. breve* (**g**) and *R. gnavus* (**h**) abundance after mouse FMT experiments (two-tailed Welch's *t* test, *n* = 5/group). Data are shown as the mean ± SEM. *P* values were determined and were indicated in each figure. ns, not

significant; *B. breve*, *Bifidobacterium breve; R. gnavus, Ruminococcus gnavus;* HC, healthy control; AD, AOM/DSS; APC, adenomatous polyposis coli; NMDS, nonmetric multidimensional scaling. Source data are provided as a Source Data file.

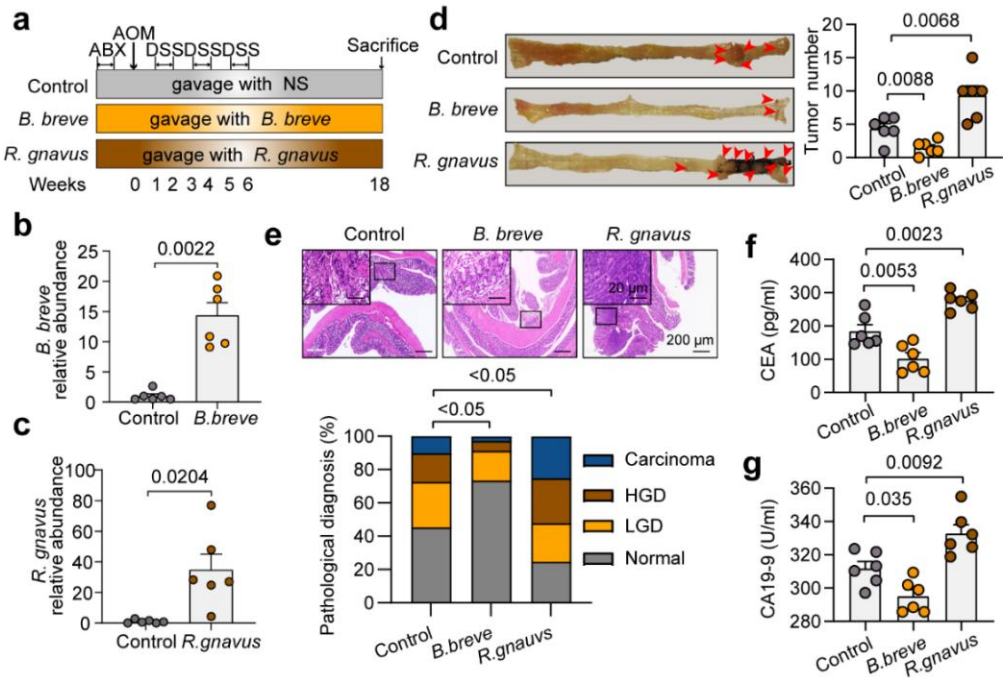

Supplementary Fig. 9. *B. breve* gavage reduces colorectal tumorigenesis, while *R. gnavus* gavage promotes colorectal tumorigenesis, related to Fig. 5. a Experimental design for mice orally gavaged with NS (control), *B. breve* or *R. gnavus*. **b** qPCR analysis of *B. breve* abundance after *B. breve* gavage experiments (two-tailed Mann-Whitney *U* test). **c** qPCR analysis of *R. gnavus* abundance after *R. gnavus* gavage treatment (two-tailed Welch's *t* test). **d** Representative colonic morphologies and average tumor number in each group. **e** Representative images of H&E staining (top) and semiquantitative analysis (bottom). H&E staining showed normal, dysplastic mucosae and carcinoma in the colon tissues. The bottom scale bar is 200 μm and the top scale bar is 20 μm. **f, g** Serum CEA (**f**) and CA19-9 levels (**g**) in each group. n = 6/group. Data are shown as the mean ± SEM. *P* values were determined by ANOVA for **d**-**g** and were indicated in each figure. NS: normal saline; ABX, antibiotic cocktail; *B. breve*, *Bifidobacterium breve; R. gnavus, Ruminococcus gnavus;* AOM, azoxymethane; DSS, dextran sodium sulfate. Source data are provided as a Source Data file.

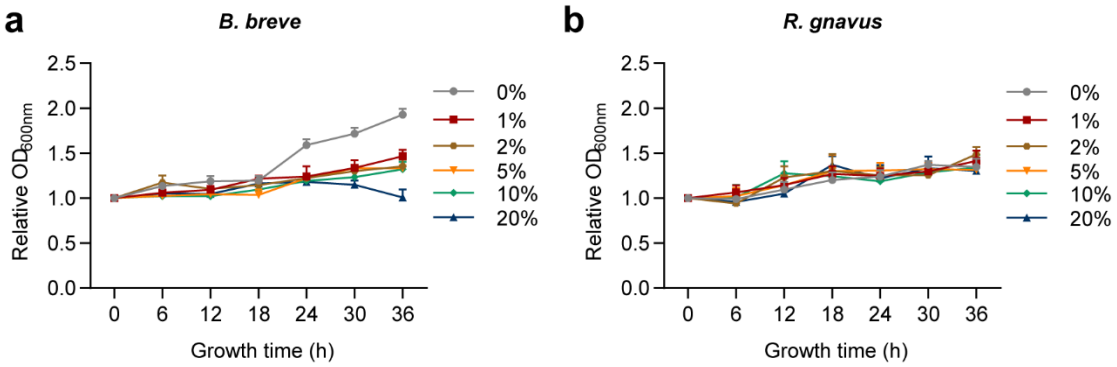

Supplementary Fig. 10. Bile acid salts alter the growth of *B. breve* and *R. gnavus*, related to Fig. 5. a Growth curve of *B. breve* after treatment with different concentrations (wt/vol) of bile acid salts. **b** Growth curve of *R. gnavus* after treatment with different concentrations (wt/vol) of bile acid salts. n = 5/group. Data are shown as the mean ± SEM. *B. breve*, *Bifidobacterium breve; R. gnavus, Ruminococcus gnavus.* All data were representative of more than three independent experiments. Source data are provided as a Source Data file.

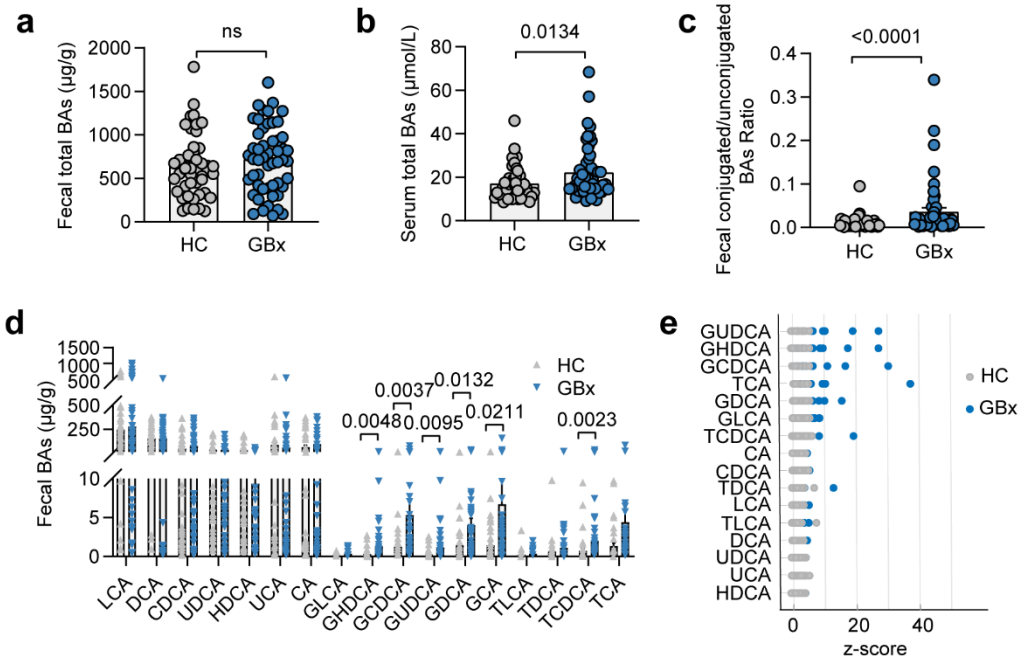

Supplementary Fig. 11. Bile acid profile in cholecystectomy patients. **a, b** Total bile acid levels in fecal (**a**) and serum (**b**) samples (n = 45 vs 52). **c** The ratio of conjugated to unconjugated bile acids in fecal samples (n = 45 vs 52). **d** Fecal bile acid profiles in the two groups (n = 45 vs 52). **e** Z-score of the fecal bile acids (n = 45 vs 52). P values were determined by two-tailed Mann Whitney U test for **a-d**. Data are shown as the mean ± SEM. P values are indicated in each figure. ns, no significant. HC, healthy control; BAs, bile acids; LCA, lithocholic acid; DCA, deoxycholic acid; CDCA, chenodeoxycholic acid; UDCA, ursodeoxycholic acid; HDCA, hyodeoxycholic acid; UCA, ursodeoxycholic acid; CA, cholic acid; GLCA, glycolithocholic acid; GHDCA, glycohyodeoxycholic acid; GCDCA, glycochenodeoxycholic acid; GUDCA, glycoursodeoxycholic acid; GDCA, glycodeoxycholic acid; GCA, glycocholic acid; TLCA, taurocholic lithocholic acid; TDCA: taurodeoxycholic acid; TCDCA, taurochenodeoxycholic acid; TCA, taurocholic acid; ns, not significant. Source data are provided as a Source Data file.

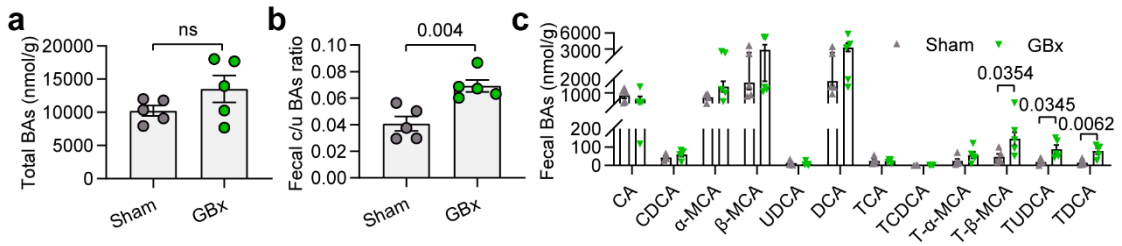

Supplementary Fig. 12. Bile acid profile in mice after cholecystectomy. a Total bile acid levels in fecal samples between the Sham and GBx mice (two-tailed *t* test). **b** The ratio of conjugated to unconjugated bile acids in fecal samples between the two groups (two-tailed *t* test). **c** Fecal bile acid profiles in the two groups (two-tailed Mann-Whitney *U* test). n = 5/group. Data are shown as the mean ± SEM. *P* values are indicated at the top of each figure. BAs, bile acids; c/u BAs, conjugated to unconjugated bile acids; CA, cholic acid; CDCA, chenodeoxycholic acid; MCA, muricholic acid; UDCA, ursodeoxycholic acid; DCA, deoxycholic acid; TCA, taurocholic acid; TCDCA, taurochenodeoxycholic acid; T-α-MCA, tauroalphamuricholic acid; T-β-MCA, taurobetamuricholic acid; TUDCA, tauroursodeoxycholic acid; TDCA, taurodeoxycholic acid; ns, not significant. Source data are provided as a Source Data file.

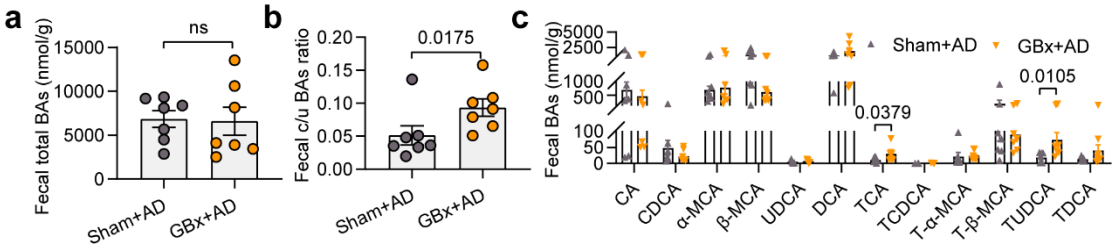

Supplementary Fig. 13. Fecal bile acid profile in mice after cholecystectomy with AOM/DSS treatment. **a** Total bile acid levels in fecal samples between the Sham+AOM/DSS and GBx+AOM/DSS mice (two-tailed *t* test). **b** The ratio of conjugated to unconjugated bile acids in fecal samples between the two groups (two-tailed Mann-Whitney *U* test). **c** Fecal bile acid profiles in the two groups (two-tailed Mann-Whitney *U* test). $n = 7$/group. Data are shown as the mean ± SEM. *P* values are indicated at the top of each figure. AD, AOM/DSS; BAs, bile acids; c/u BAs, conjugated to unconjugated bile acids; ns, not significant; CA, cholic acid; CDCA, chenodeoxycholic acid; MCA, muricholic acid; UDCA, ursodeoxycholic acid; DCA, deoxycholic acid; TCA, taurocholic acid; TCDCA, taurochenodeoxycholic acid; T-α-MCA, tauroalphamuricholic acid; T-β-MCA, taurobetamuricholic acid; TUDCA, tauroursodeoxycholic acid; TDCA, taurodeoxycholic acid. Source data are provided as a Source Data file.

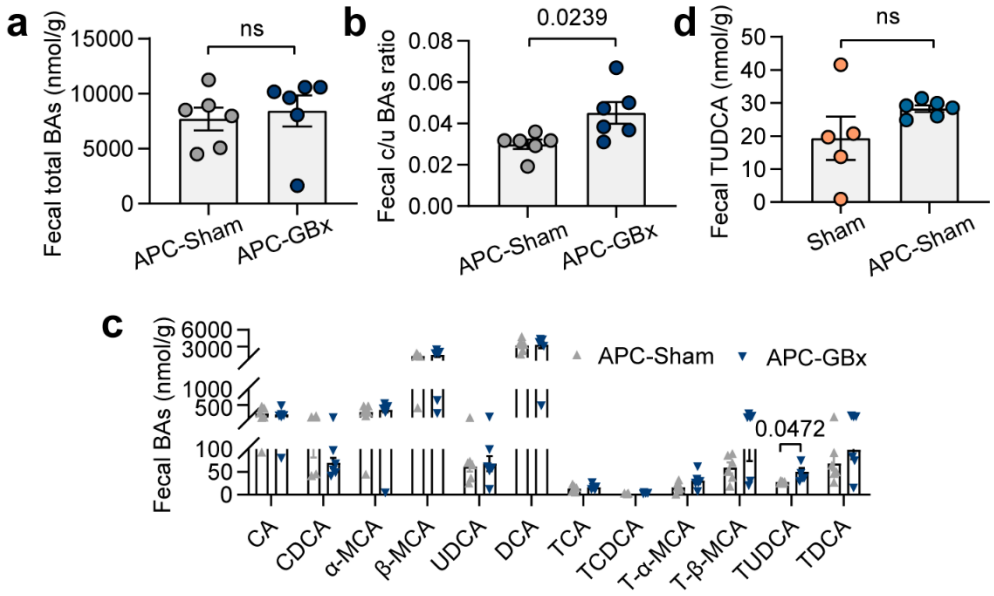

Supplementary Fig. 14. Bile acid profile after cholecystectomy in APC$^{min/+}$ mice, and fecal level of TUDCA between Sham and APC-Sham groups. **a** Total bile acid levels in fecal samples of APC$^{min/+}$ mice with or without cholecystectomy (two-tailed Mann-Whitney *U* test, *n* = 6/group). **b** The ratio of conjugated to unconjugated bile acids in fecal samples between the two groups (two-tailed *t* test, *n* = 6/group). **c** Fecal bile acid profiles in the two groups (two-tailed Mann-Whitney *U* test, *n* = 6/group). **d** Fecal TUDCA level between Sham and APC-Sham groups (two-tailed Welch's *t* test, *n* = 5 vs 6). Data are shown as the mean ± SEM. *P* values for each test were determined and indicated in each figure. APC, adenomatous polyposis coli; BAs, bile acids; c/u BAs, conjugated to unconjugated bile acids; CA, cholic acid; CDCA, chenodeoxycholic acid; MCA, muricholic acid; UDCA, ursodeoxycholic acid; DCA, deoxycholic acid; TCA, taurocholic acid; TCDCA, taurochenodeoxycholic acid; T-α-MCA, tauroalphamuricholic acid; T-β-MCA, taurobetamuricholic acid; TUDCA, tauroursodeoxycholic acid; TDCA, taurodeoxycholic acid; ns, not significant. Source data are provided as a Source Data file.

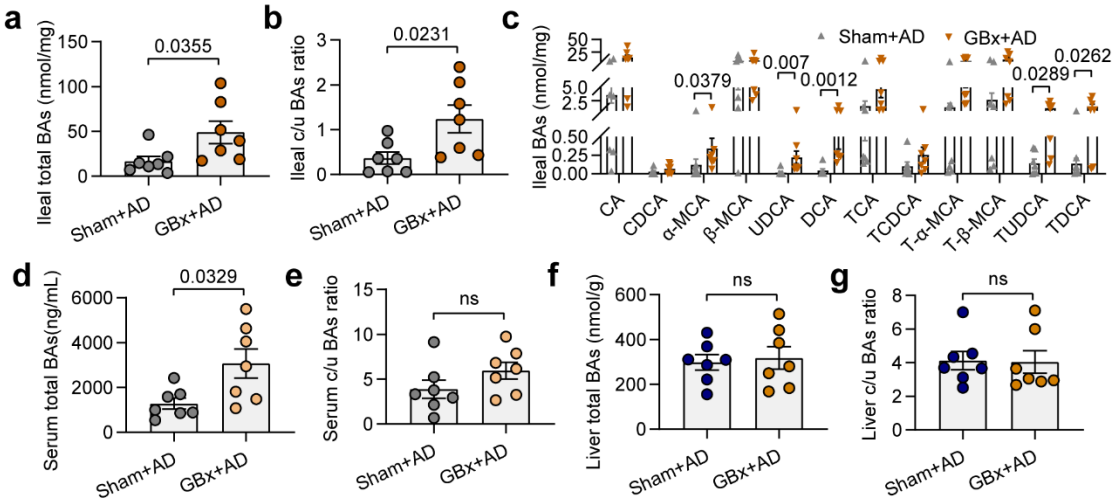

Supplementary Fig. 15. Bile acid profile in mice after cholecystectomy with AOM/DSS treatment. **a** Total bile acid levels in the distal ileum between the Sham+AOM/DSS and GBx+AOM/DSS mice. **b** The ratio of conjugated to unconjugated bile acids in the distal ileum between the two groups. **c** Ileal bile acid profiles in the two groups (two-tailed Mann-Whitney *U* test). **d** Total bile acid levels in serum samples between the Sham+AOM/DSS and GBx+AOM/DSS mice (two-tailed Welch's *t* test). **e** The ratio of conjugated to unconjugated bile acids in serum samples between the two groups. **f** Total bile acid levels in liver samples between the Sham+AOM/DSS and GBx+AOM/DSS mice. **g** The ratio of conjugated to unconjugated bile acids in liver samples between the two groups (two-tailed Mann-Whitney *U* test). n = 7/group. Data are shown as the mean ± SEM. *P* values were determined by two-tailed *t* test for **a, b, e** and **f,** and were indicated in each figure. AD, AOM/DSS; BAs, bile acids; c/u BAs, conjugated to unconjugated bile acids; ns, not significant. Source data are provided as a Source Data file.

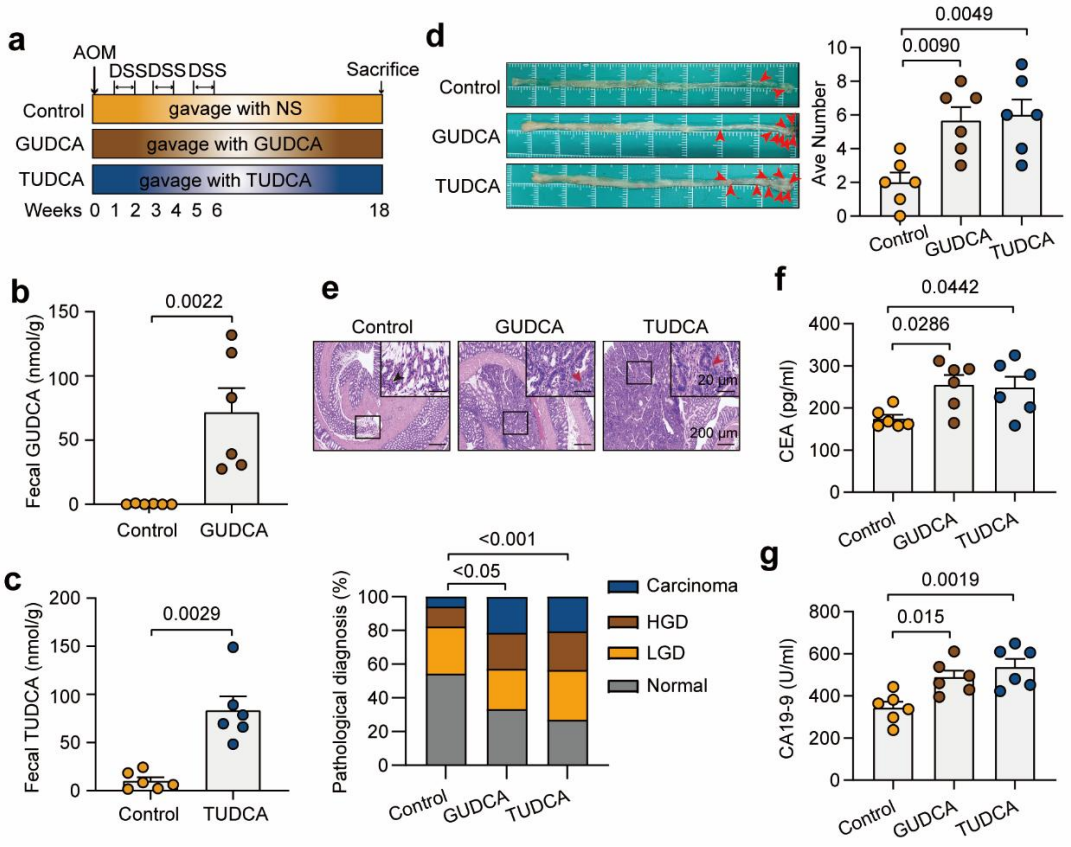

Supplementary Fig. 16. GUDCA and TUDCA gavage promotes colorectal tumorigenesis, related to Fig. 5. a Experimental design for mice orally gavaged with NS (control), GUDCA or TUDCA. **b** Fecal GUDCA level after GUDCA gavage (two-tailed Mann-Whitney *U* test). **c** Fecal TUDCA level after TUDCA gavage (two-tailed Welch's *t* test). **d** Representative colonic morphologies and average tumor number in each group. **e** Representative images of H&E staining (top) and semiquantitative analysis (bottom). H&E staining showed normal, dysplastic mucosae and carcinoma in the colon tissues. The regions of the lesion were pointed out by arrows. black arrows: dysplastic mucosae; red arrows: carcinoma. The bottom scale bar is 200 μm and the top scale bar is 20 μm. **f, g** Serum CEA **(f)** and CA19-9 levels **(g)** in each group. n = 6/group. Data are shown as the mean ± SEM. *P* values were determined by ANOVA for **d-g** and were indicated in each figure. NS: normal saline; GUDCA, glycoursodeoxycholic acid;

TUDCA, tauroursodeoxycholic acid; AOM, azoxymethane; DSS, dextran sodium sulfate. Source data are provided as a Source Data file.

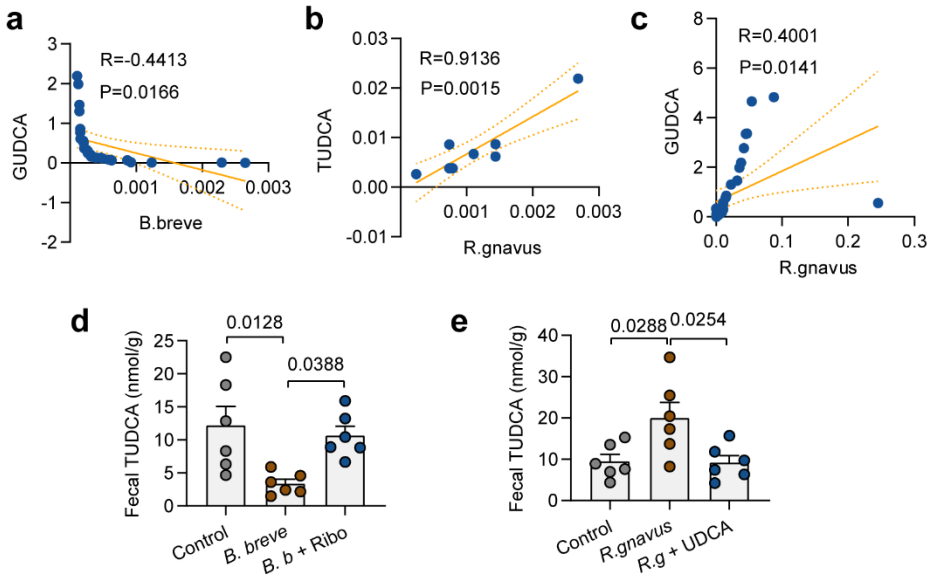

Supplementary Fig. 17. The correlations of *B. breve* and *R. gnavus* with bile acids, and the fecal level of TUDCA with inhibitors administration, related to Fig. 5. a The correlation of *B. breve* with the levels of GUDCA in patients with cholecystectomy. **b** The correlation of *R. gnavus* with the levels of TUDCA in mice with cholecystectomy after AOM/DSS treatment. **c** The correlation of *R. gnavus* with the levels of GUDCA in patients with cholecystectomy. The correlations were determined by Pearson correlation analysis. **d** Fecal TUDCA level after *B. breve* gavage with or without riboflavin. **e** Fecal level of TUDCA following the gavage of *R. gnavus* in the presence or absence of UDCA. n = 6/group for **d-e**. Data are shown as the mean ± SEM. *P* values were determined by ANOVA for **d-e** and were indicated in each figure. Ribo, riboflavin. Source data are provided as a Source Data file.

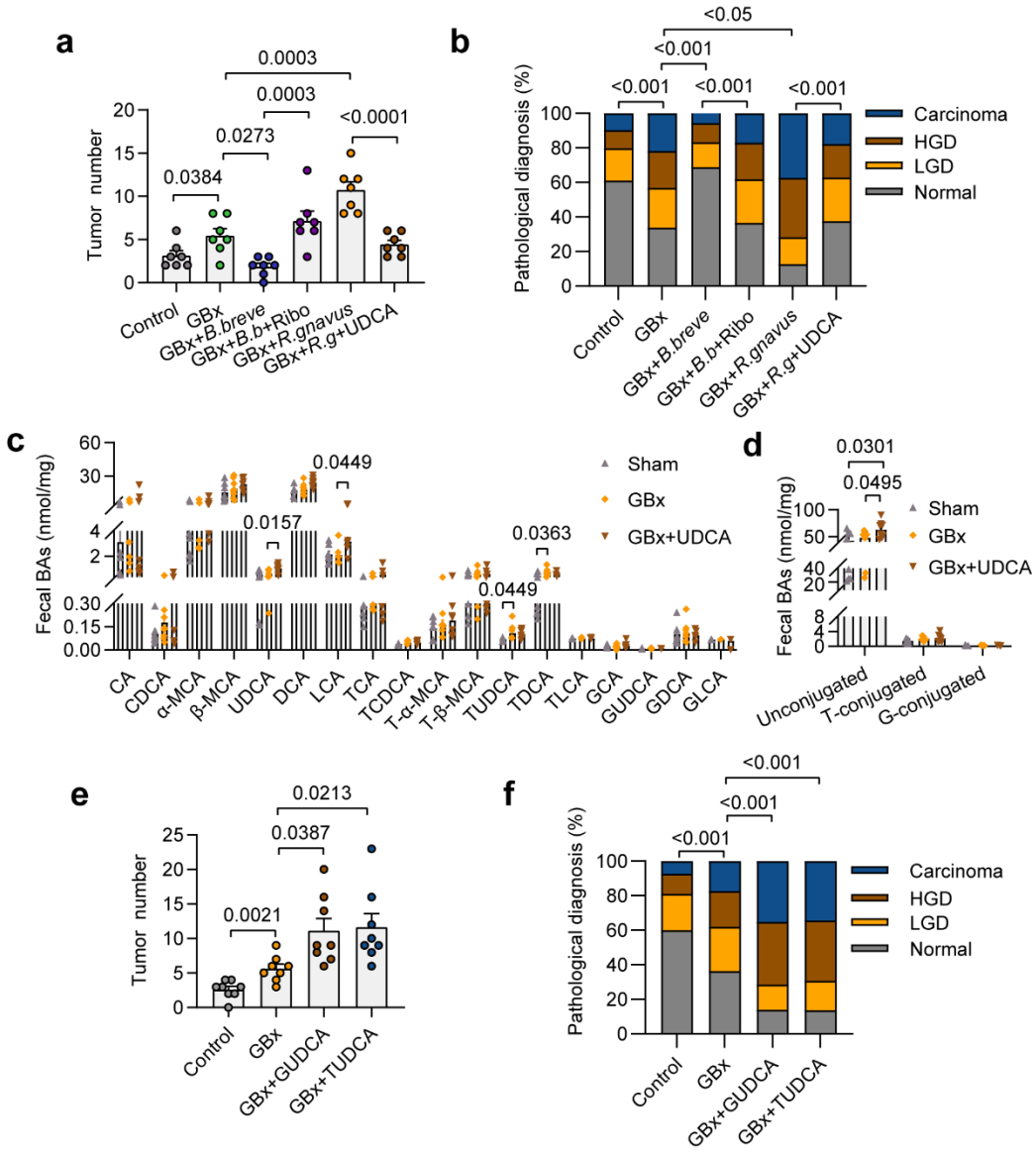

Supplementary Fig. 18. Tumor number and quantitative analysis of H&E staining in mice, as well as the bile acid profile in GBx mice treated with UDCA after AOM/DSS treatment, related to Fig. 5. a Average tumor number in mice after *B. breve* or *R. gnavus* gavage, treated with the BSH inhibitor riboflavin or the 7β-HSDH inhibitor UDCA, respectively (n = 7/group). **b** Quantitative analysis of H&E staining in each group (n = 7/group). **c** Fecal bile acid profiles in GBx mice with or without UDCA treatment (n = 8/group). **d** Unconjugated and conjugated bile acids in fecal samples of each group (n = 8/group). **e** Average tumor number in mice treated with

GUDCA or TUDCA after establishing the AOM/DSS model (n = 8/group). **f** Quantitative analysis of H&E staining in each group (n = 8/group). Data are shown as the mean ± SEM. P values were determined by ANOVA and were indicated in each figure. Ribo, riboflavin. Source data are provided as a Source Data file.

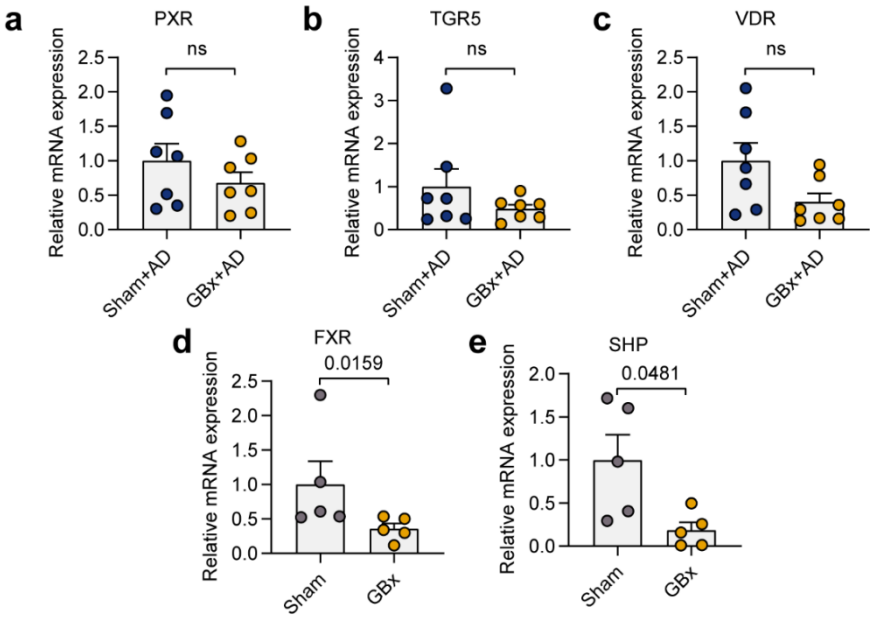

Supplementary Fig. 19. The relative expression of bile acid receptors in Sham and GBx mice with or without AOM/DSS treatment, related to Fig. 6. a Relative expression of PXR within the colon cancerous tissues from Sham+AOM/DSS and GBx+AOM/DSS mice (two-tailed *t* test, *n* = 7/group). **b** Relative expression of TGR5 in colon cancerous tissues obtained from mice treated with AOM/DSS treatment (two-tailed Mann-Whitney *U* test, *n* = 7/group). **c** The relative expression levels of VDR in colon cancerous tissues of each group (two-tailed *t* test, *n* = 7/group). **d** Relative expression of FXR in the colon tissues of Sham and GBx mice (two-tailed Mann-Whitney *U* test, *n* = 5/group). **e** The relative expression level of SHP in the colon tissues of each group (two-tailed Welch's *t* test, *n* = 5/group). Data are shown as the mean ± SEM. *P* values are indicated in each figure. All data were representative of more than three independent experiments. PXR, pregnane X receptor; TGR5, Takeda G protein-coupled receptor 5; VDR, vitamin D receptor; FXR, farnesoid X receptor; SHP, small heterodimer partner; ns, not significant. Source data are provided as a Source Data file.

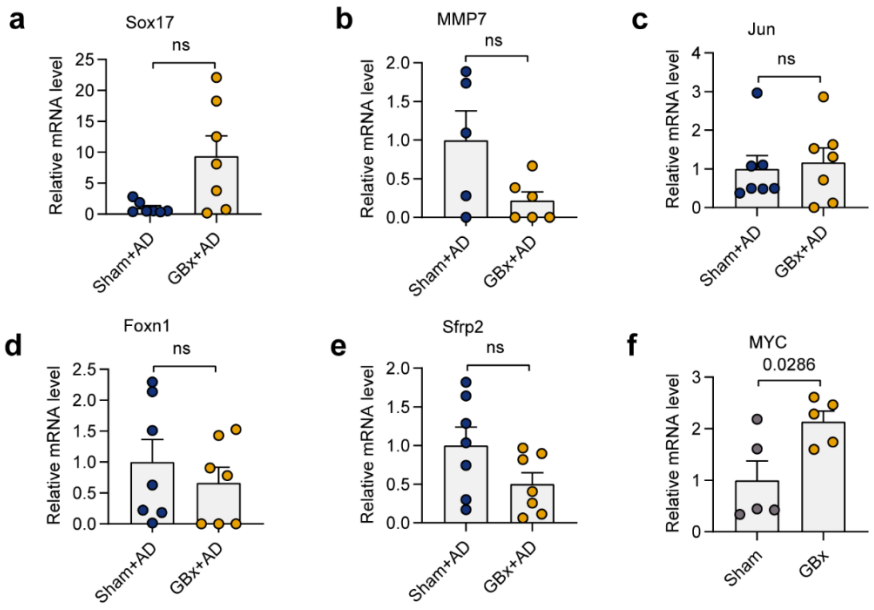

Supplementary Fig. 20. The relative expression of target genes of Wnt/β-catenin signaling in GBx mice after AOM/DSS treatment, related to Fig. 6. a Relative expression of Sox17 in the colon cancerous tissues derived from Sham+AOM/DSS and GBx+AOM/DSS mice (two-tailed Mann-Whitney *U* test, *n* = 7/group). **b** Relative expression levels of Mmp7 in the colon cancerous tissues of mice after AOM/DSS treatment (two-tailed Welch's *t* test, *n* = 5 vs 6). **c** Relative expression of Jun in the colon cancerous tissues of each group (two-tailed Mann-Whitney *U* test, *n* = 7/group). **d** The relative expression levels of Foxn1 in the colon cancerous tissues of each group (*n* = 7/group). **e** Relative expression of Sfrp2 in the colon cancerous tissues of each group (*n* = 7/group). **f** The relative expression of MYC in the colon tissues from Sham and GBx mice (*n* = 5/group). Data are shown as the mean ± SEM. *P* values were determined by two-tailed *t* test for **d**-**f**, and were indicated in each figure. Sox 17, SRY-box transcription factor 17; Mmp7, matrix metallopeptidase 7; Jun, jun proto-oncogene; Foxn1, forkhead box N1; Sfrp2, secreted frizzled-related protein 2; ns, not significant. Source data are provided as a Source Data file.

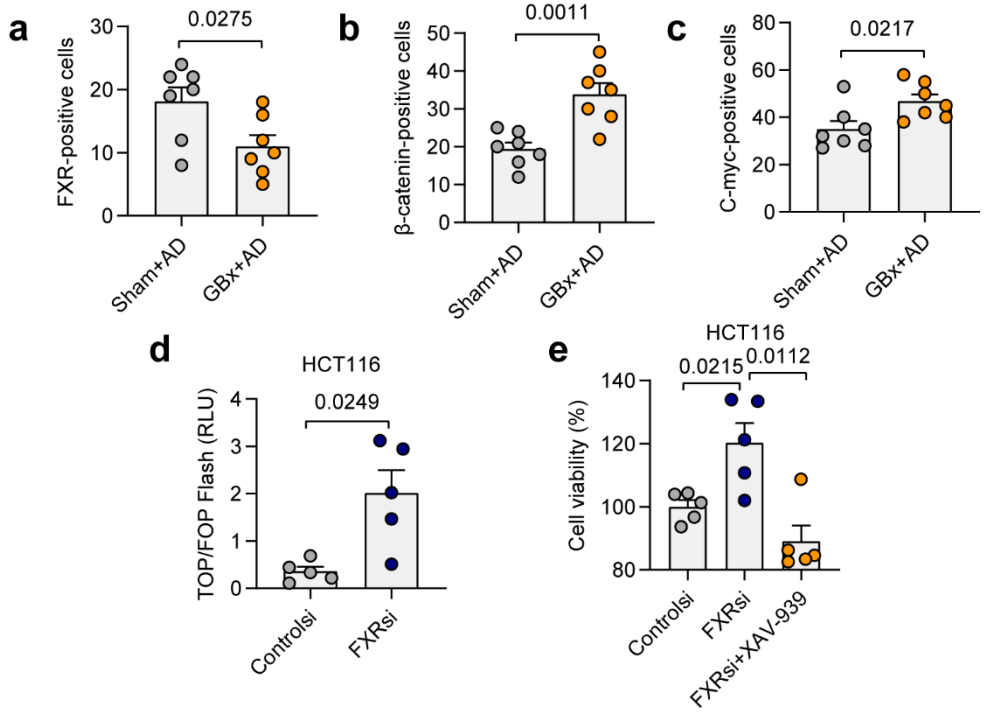

Supplementary Fig. 21. FXR/β-catenin signaling is involved in colorectal tumorigenesis induced by cholecystectomy, related to Fig. 6. **a-c** Quantitative analysis of FXR (**a**), β-catenin (**b**), and c-Myc (**c**) immunohistochemistry staining in Sham+AOM/DSS or GBx+AOM/DSS mice (n = 7/group). **d** The effect of FXR knockdown on the luciferase activity of TOP/FOP-Flash reporter plasmid in HCT116 cells (two-tailed Welch's t test, n = 5/group). **e** The effect of FXR knockdown and XAV939 on the viability of colon cancer cells detected by CCK8 assays (ANOVA, n = 5/group). Data are shown as the mean ± SEM. P values were determined by two-tailed t test for **a-c**, and were indicated in each figure. All data were representative of more than three independent experiments. Source data are provided as a Source Data file.

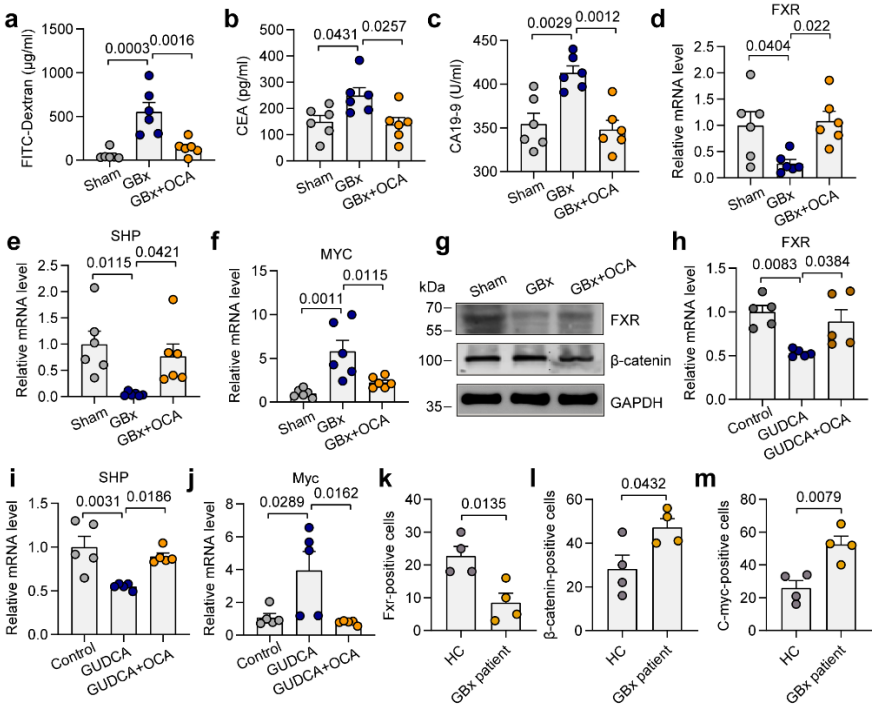

Supplementary Fig. 22. FXR/β-catenin signaling is altered after OCA treatment in GBx mice or GUDCA-treated intestinal organoids, related to Fig.7. a Intestinal permeability measured by FITC-dextran in GBx+AOM/DSS mice treated with OCA (*n* = 6/group). **b, c** Serum CEA (**b**) and CA19-9 (**c**) levels in each group (*n* = 6/group). **d-f** Relative expression of FXR (**d**), SHP (**e**), and MYC (**f**) in the colon cancerous tissues of each group (*n* = 6/group). **g** Protein expression of FXR and GAPDH in the colon tissues in each group. **h-j** Relative expression of FXR (**h**), SHP (**i**), and MYC (**j**) in intestinal organoid treated with GUDCA and OCA (*n* = 5/group). **k-m** Quantitative analysis of FXR (**k**), β-catenin (**l**), and c-Myc (**m**) IHC staining in the colon tissues obtained from healthy controls and patients with cholecystectomy (two-tailed *t* test, *n* = 4/group). Data are shown as the mean ± SEM. *P* values were determined by ANOVA for **a-f, h-j** and were indicated in each figure. HC, healthy control; GBx, cholecystectomy; OCA, obeticholic acid. All data were representative of more than three independent experiments. Source data are provided as a Source Data file.

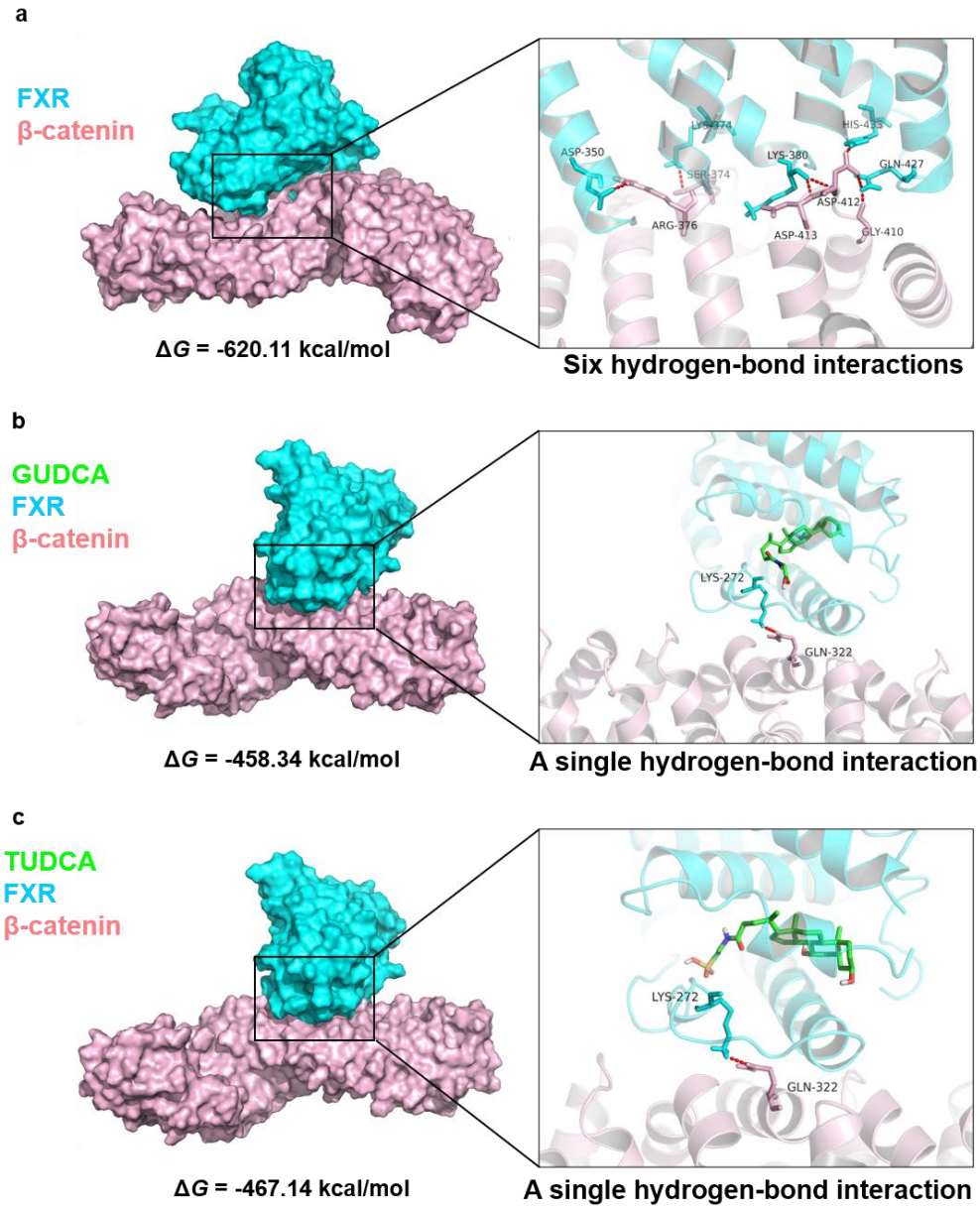

Supplementary Fig. 23. Molecular docking of the interaction between FXR and β-catenin. a Docking of the apo-FXR (PDB: 5Q0K) into the β-catenin (PDB: 1JDH). **b** Docking of the GUDCA/FXR (PDB: 4WVD) into the β-catenin (PDB: 1JDH). **c** Docking of the TUDCA/FXR (PDB: 4WVD) into the β-catenin (PDB: 1JDH). The FXR was colored cyan, and the β-catenin was colored pink. The hydrogen bonds were indicated with red dashed lines. GUDCA, TUDCA and residues contributing hydrogen bonds were highlighted as stick models.

Supplementary Tables

Supplementary Table 1. Demographic and clinical characteristics of healthy controls and cholecystectomy patients

Parameter	Healthy (N=45)	Cholecystectomy (N=52)	*P* Value
Gender, female, No, (%)	28 (62.22%)	32 (61.54%)	0.95
Age (years)	48.53±1.31	51.15±1.42	0.68
Postoperative time (years)		9.08±0.83	
Height (m)	1.62±1.28	1.61±1.18	0.85
Weight (Kg)	55.24±1.34	55.13±1.25	0.76
BMI (Kg/m^2)	24.91±0.41	25.30±0.26	0.63
Clinical symptoms			
Acid Reflux, No. (%)	4 (8.89%)	5 (9.62%)	0.90
Diarrhea, No. (%)	2 (4.44%)	10 (19.23%)	0.03
Abdominal Distension, No. (%)	5 (11.11%)	7 (13.46%)	0.73
Abdominal Pain, No. (%)	2 (4.44%)	8 (15.38%)	0.08
Constipation, No. (%)	3 (6.67%)	4 (7.69%)	0.85
Liver function test			
ALT (U/L)	22.39±1.55	28.40±3.09	0.53
AST (U/L)	22.16±1.05	24.37±1.22	0.66
ALP (U/L)	87.90±3.52	90.89±4.89	0.41
GGT(U/L)	24.66±1.99	30.93±2.45	0.29
TBIL(μmol/L)	10.03±0.75	10.66±0.60	0.24
Comorbidities			
HBP, No. (%)	8 (17.78%)	10 (19.23%)	0.85
HLP, No. (%)	5 (11.11%)	7 (13.46%)	0.73
DM, No. (%)	3 (6.67%)	6 (11.54%)	0.41
MAFLD, No. (%)	3 (6.67%)	4 (7.69%)	0.85
AILD, No. (%)	1 (2.22%)	2 (3.85%)	0.65
Cirrhosis, No. (%)	0 (0.00%)	1 (1.92%)	0.35
IBD, No. (%)	1 (2.22%)	2(3.85%)	0.65
CRC, No. (%)	0 (0.00%)	2 (3.85%)	0.18

Data were presented as the Mean ± SE, *P* values were determined by chi-square test. ALT, alanine aminotransferase; AST, aspartate aminotransferase; ALP, alkaline phosphatase; GGT, gamma-glutamyl transferase; TBIL, total bilirubin; HBP, high blood pressure; HLP, hyperlipidemia; DM, diabetes; MAFLD, metabolic dysfunction-associated fatty liver disease; AILD, autoimmune liver disease; IBD, inflammatory bowel disease; CRC, colorectal cancer. Source data are provided as a Source Data file.

Supplementary Table 2. Primers for colon tissues RT-PCR

Gene name	Forward primer (5'→3')	Reverse primer ((5'→3')
Foxn1	CTGCTCGTCGTTTGTGCCT	TGCCTCTTGTAGGGGTGGAAA
Jun	TTCCTCCAGTCCGAGAGCG	TGAGAAGGTCCGAGTTCTTGG
Mmp7	CTTACCTCGGATCGTAGTGGA	CCCCAACTAACCCTCTTGAAGT
Myc	ATGCCCCTCAACGTGAACTTC	GTCGCAGATGAAATAGGGCTG
Sfrp2	GCCAGCCCGACTTCTCCTA	CCGCATGTTCTGGTACTCGAT
Sox17	GATGCGGGATACGCCAGTG	CCACCTCGCCTTTCACCTTTA
FXR	TGGGCTCCGAATCCTCTTAGA	TGGTCCTCAAATAAGATCCTTGG
SHP	TCTGCAGGTCGTCCGACTATTC	AGGCAGTGGCTGTGAGATGC
TGR5	TGCTTCTTCCTAAGCCTACTACT	CTGATGGTTCCGGCTCCATAG
VDR	GAATGTGCCTCGGATCTGTGG	ATGCGGCAATCTCCATTGAAG
PXR	CCCATCAACGTAGAGGAGGA	GGGGGTTGGTAGTTCCAGAT
ZO-1	GCCGCTAAGAGCACAGCAA	GCCCTCCTTTTAACACATCAGA
Occludin	TGAAAGTCCACCTCCTTACAGA	CCGGATAAAAAGAGTACGCTGG
IL-1β	GAAATGCCACCTTTTGACAGTG	TGGATGCTCTCATCAGGACAG
TNF-α	CAGGCGGTGCCTATGTCTC	CGATCACCCCGAAGTTCAGTAG
GAPDH	ACCCAGAAGACTGTGGATGG	CACATTGGGGGTAGGAACAC

Supplementary Table 3. Primers used to quantify bacteria by qPCR

Target (16S rRNA gene of :)	**Primer name**	**Sequence**
B. breve	16SBbF	TAGGGAGCAAGGCACTTTGTGT
	16SBbR	ATCCGAACTGAGACCGGTT
R. gnavus	16SRgF	TGGCGGCGTGCTTAACA
	16SRgR	TCCGAAGAAATCCGTCAAGGT
All bacteria	UniF	GTGSTGCAYGGYYGTCGTCA
	UniR	ACGTCRTCCMCNCCTTCCTC